Program Digest, 2019 IEEE International Ultrasonics Symposium (IUS)
Glasgow, Scotland, October 6-9, 2019

Liquid operable AlN PMUT with high output pressure capabilities

E. Ledesma
Electronics Eng. Dept.
Universitat Autónoma de Barcelona
Bellaterra, Spain
eyglis.ledesma@uab.cat

I.Zamora
Electronics Eng. Dept.
Universitat Autónoma de Barcelona
Bellaterra, Spain
ivan.zamora@uab.cat

V.Tzanov
Electronics Eng. Dept.
Universitat Autónoma de Barcelona
Bellaterra, Spain
vassil.tzanov@uab.cat

F.Torres
Electronics Eng. Dept.
Universitat Autónoma de Barcelona
Bellaterra, Spain
francesc.torres@uab.cat

A.Uranga
Electronics Eng. Dept.
Universitat Autónoma de Barcelona
Bellaterra, Spain
arantxa.uranga@uab.cat

N.Barniol
Electronics Eng. Dept..
Universitat Autónoma de Barcelona
Bellaterra, Spain
nuria.barniol@uab.cat

E.Marigó
Silterra Malaysia Sdn. Bhd.
Kulim, Malaysia
eloi_marigo@silterra.com

Mohan Soundara-Pandian
Silterra Malaysia Sdn. Bhd.
Kulim, Malaysia
mohanraj_soundara
@silterra.com

***Abstract*—Two piezoelectric micromachined ultrasonic transducers (PMUTs) with a mode shape like a free membrane and a resonance frequency around 7 MHz in liquid environment are proposed in this paper. Here we evaluate the influence of linear holes (two or four holes) in the movement and consequently in the output pressure. FEM simulations show how the linear holes increase the membrane velocity at least 1.4x factor in relation with the clamped PMUT. Also, the experimental verification in fluorinert (FC-70) allows to demonstrate the capability to use them in liquid with an output surface pressure in the range of 300 Pa/V at 7 MHz.**

Keywords—* *piezoelectric micromachined ultrasonic transducer, PMUT, CMOS-MEMS, AlN, acoustic pressure.

I. Introduction

New piezoelectric micromachined ultrasonic transducers (PMUTs) with high output pressure, high frequency and small size are needed for producing high-quality ultrasound imaging systems. Considering 500 dpi images, operation in liquid environment (sound velocities around 1000 m/s), a pixel size below 50 µm will be desired with operation frequencies higher than 5 MHz for 100 µm axial resolution [1].

Conventional PMUTs are based on suspended piezoelectrical flexural membranes fully clamped deviating from a piston-like movement with a clear reduction of the membrane displacement and output pressure. Additionally, these clamped membranes suffer from residual, and due to only 1/3 of the total area moves with uniform velocity, the effective area is Total-Area/3, as consequence, the output acoustic pressure is considerably affected. To avoid this, reported works propose piston-like motion membranes, such as suspended membranes, to obtain higher displacements [2][3][4]. However, these structures do not work properly in liquid environment due to the filling of the cavity through the opened etching holes.

In this paper we propose two different piston-like PMUTs, the first one with linear holes on the 4 sides (tent-plate) and the second one with 2 sides (bridge structure) which are compared with a standard clamped PMUT, with resonance frequencies higher than 5 MHz and efficiently operated in liquid environment.

II. PMUTs Device

Clamped and tent-plate are squared AlN PMUT with 40 µm side, while bridge PMUT measures 40 µm x 47 µm, the layout for these devices is showing in Fig. 1. The clamped PMUT has 8 etching structures out of the PMUT-body; tent-plate is clamped only in the corners due to four linear holes (2 µm x 26 µm) and bridge structure is asymmetric with two linear of 2 µm x 40 µm.

All PMUTs have a 1.3 µm AlN piezoelectric material, and 1.5 µm Si_3N_4 passive layer which acts as the elastic layer and seals the cavity. The electrodes are Al and have 0.35 µm top and 0.40 µm bottom. The MEMS-on-CMOS process from Silterra has been used to fabricate these PMUTs and it has been reported in previously works [5][6][7].

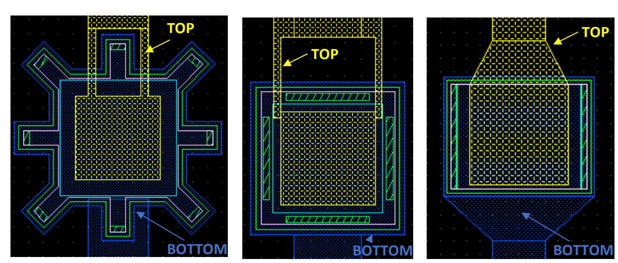

Fig. 1. Layout of the three PMUTs: clamped (left); tent-plate (middle); bridge (right). Yellow layer is the top electrode and blue layer is the bottom electrode.

III. Simulation Results

Mechanical simulations with the FEM simulator COMSOL Multiphysics have been done. Fig. 2 shows the static displacement of the membrane for the three designs PMUTs. Clamped PMUT exhibits a Gaussian mode shape. On the other site, tent-plate PMUT, and more evident bridged PMUT (at the non-clamped site) present a close piston-like mode shape. Comparing the maximum displacement at the center of the membrane, it is clearly shown a considerable improvement in the tent-plate PMUT in contrast with the standard PMUT, a 2.4x factor (tent-plate) and 1.7x factor (bridge) better. These simulations also show an asymmetry in the x-direction displacement of the bridged PMUT (black curve in Fig. 2). This asymmetry is caused by the top electrode which is connected to the substrate in only one site (see Fig. 1). From these simulations it can be concluded that the tent-plate PMUT is expected to produce higher output pressures than the other two designs. In order to verify this, dynamic simulations with COMSOL under liquid environment has been performed for the three designed PMUTs.

The output pressure in far field is given by (1) where c is the sound velocity in the medium, ρ its density, υ the membrane velocity, R_0 is the Rayleigh distance (R_0=PMUT surface/wavelength), z the axial position and P_0 is called surface pressure.

$$P(z) = c*\rho*\upsilon*R_0/z = P_0*R_0/z \quad (1)$$

From this equation, it is seen that the surface pressure is directly proportional to the membrane velocity. For this reason, normalized membrane velocity with the applied voltage was computed from the FEM dynamic simulations according to (2):

$$\upsilon = 2*\pi*f*ds/V \quad (2)$$

where f is the simulated resonance frequency, ds is the simulated center-displacement and V is the applied voltage. Table I shows the results in fluorinert (FC-70). The clamped PMUT exhibits the higher frequency while the higher velocity is found for the tent-plate PMUT in the first place and bridge is in second place: 7.22 mm/s*V^{-1} and 4.63 mm/s*V^{-1} respectively, achieving 2.16x and 1.4x enhancement in relation with a conventional PMUT (3,33 mm/sV^{-1}).

These dynamic simulations are in accordance with the static deflection computed and shown in Fig. 2, for the tent-plate PMUT despite its lower resonance frequency. These simulations demonstrate the positive influence of the holes in the performance of the PMUTs.

TABLE I. Dynamic simulated membrane velocity of the PMUTs in FC-70

Devices	*Displacement at center per volt (nm/V)*	*Frequency (MHz)*	*Normalized Membrane velocity (mm/s*V^{-1})*
Tent-Plate	0.1184	9.7	7.22
Clamped	0.0442	12	3.33
Bridge	0.1038	7.1	4.63

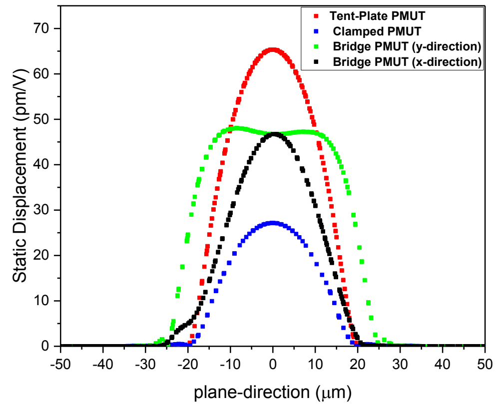

Fig. 2. Static displacement of the three PMUTs in x and y directions: tent-plate (red curve in both directions); clamped (blue curve in both directions); bridge (green curve for y-direction: it cuts free sides and black curve for x-direction: it cuts the clamped side).

IV. Experimental Characterization

A. Electrical measurements

Fig. 3 shows the optical image of the PMUTs described in this paper. The electrical measurements in air were done using the probe table and network analyzer obtaining 20 MHz, 16 MHz and 18.5 MHz for tent-plate, bridge and clamped PMUT respectively. The resonance frequency in FC-70 is estimated using (3):

$$f_{FC\text{-}70} = f_{air}/\sqrt{(1+\beta)} \quad (3)$$

where f_{air} is the obtained electrical measurement and β is the added virtual mass factor [8]. The resonances frequencies predicted by this model in FC-70 are 8.35 MHz for tent-plate, 7.73MHz for clamped and 6.68 MHz for bridge.

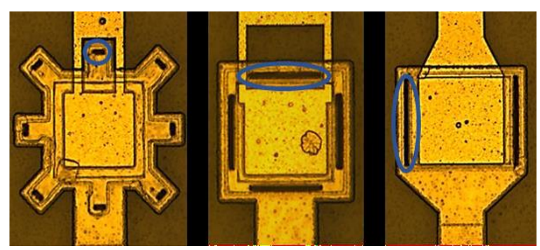

Fig. 3. Optical image of the three PMUTs: clamped (left); tent-plate (middle); bridge (right). Blue circles are drawn over individual sealed holes for each design.

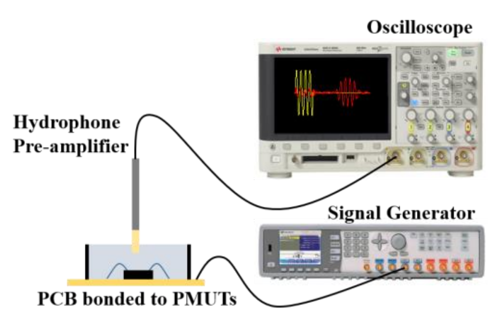

Fig. 4. Setup for the acoustic measurements as actuator.

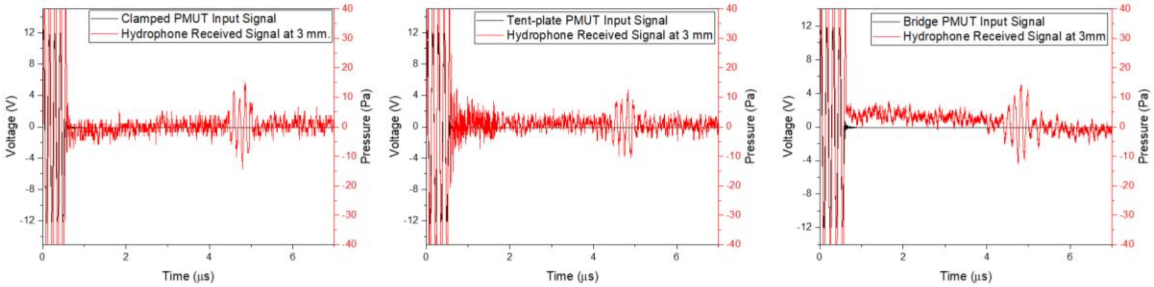

Fig. 5: Acoustic pressure measured in FC-70 at 3 mm over PMUT surface: clamped (left); tent-plate (middle); bridge (right)

B. Acoustic measurements

The acoustic characterization as actuator has been doing in fluorinert (FC-70, with c = ~680 m/s and ρ = 1940 kg/m^3) using a hydrophone from ONDA, HNC-1500, calibrated in water. PMUTs were driven with 4 cycles with 22.3 Vpp at the resonance frequencies for these devices in FC-70, and the signal was acquired 3 mm over the PMUTs surface, see setup in Fig. 4 and the time domain obtained response in Fig. 5.

From the acquired voltage amplitude and considering the hydrophone calibration, the pressure at 3 mm and the surface pressure, P_0 (using (1) and normalizing with respect to 22.3 Vpp applied voltage), for each of the PMUTs designs are obtained (see Table II).

All PMUTs exhibit the maximum acoustic response at a resonance frequency around 7 MHz, in accordance to (3) and below the simulated ones. In fact, and due to the wide frequency bandwidth of the PMUTs in liquid operation, there is a small dependence of the acquired voltage from the hydrophone with a change in the actuation frequency of the PMUT. This makes the determination of the experimental resonance frequency not very accurate.

On the other site, both the output pressure at 3 mm as well as the surface pressure are unexpectedly very close for the three designed PMUTs, between 30-40 Pa and around 320 Pa/V (averaged value) respectively, and not showing significant variations as was expected from the simulations (see for instance displacement in Fig. 1). This discrepancy between simulation and experimental results is due to the modelization of the PMUTs which does not consider the conformality of the different layers of the PMUT and specially the conformality of the passive layer for the tent-plate and bridged PMUTs. We have presented elsewhere simulations showing the importance to take into account this conformality in the different layers of the PMUT to obtain more accurate results from the simulation. As a consequence of the obtained experimental output pressures, it cannot be set differences between the three designed PMUTs. On the other hand, it can be said that the PMUTs presented in this paper are very competitive in comparison with the ones published in the literature using AlN as piezoelectric material. For instance, a recent published low-thermal AlN PMUT in liquid operation reports values of 2.93 kPa/V @ 5.5 MHz with an array of 3x20 short-circuited PMUTs [9]. Normalizing this value to a single PMUT, the surface pressure would be 48 Pa/V,

TABLE II. PERFORMANCE OF THE PMUTS IN FC-70 AS ACTUATOR.

Devices	*Acquired peak-to-peak voltage (µVpp)*	*Frequency (MHz)*	*Pressure @ 3mm Pa*	*Surface pressure, P_0 Pa/V*
Tent-Plate	280 ± 43	7.4	39 ± 6	340 ± 52
Clamped	200 ± 50	7.5	28 ± 7	260 ± 65
Bridge	400 ± 33	6.7	44 ± 3	360 ± 30

which is a 7.5x factor lower than the presented here for the bridged PMUT, demonstrating the capabilities of the presented designs.

CONCLUSIONS

In this work, the FEM simulations and the acoustic characterizations of different PMUTs designs with piston-like shape and operable in liquid have been done. The operation in liquid is due to the passive layer sealing of the etching holes for releasing the PMUT. Simulations demonstrate better behavior in the tent-plate and bridged PMUT than the clamped membrane. Despite of this, dispersion on the experimental results are not conclusive in this comparison, giving similar results for the standard clamped design and the new proposed ones. The influence of the holes filling due to the conformal deposition of the passive-sealing layer affects the predicted behavior and degrades the expected and simulated behavior. Some fabrication process modifications would alleviate this degradation and exploit the benefits of the tent-plate and bridge PMUTs proposed. In any case, all the fabricated PMUTs provide an output surface pressure around 300 Pa/V at 7 MHz which is a very competitive value in comparison with other reported using AlN piezoelectric material compatible with CMOS technology.

ACKNOWLEDGMENT

This work has been partially supported by project TEC2015-66337-R (MINECO/FEDER).

REFERENCES

[1] X. Jiang et al., "Monolithic 591×438 DPI ultrasonic fingerprint sensor," Proc. IEEE Int. Conf. Micro Electro Mech. Syst., vol. 2016-Febru, no. January, pp. 107–110, 2016.

[2] Y. Liang, B. E. Eovino, and L. Lin, "Pinned Boundary Piezoelectric Micromachined Ultrasonic Transducers," in IEEE MEMS, 2019, no. January, pp. 791–794.

[3] T. Wang, R. Sawada, and C. Lee, "A piezoelectric micromachined ultrasonic transducer using piston-like membrane motion," IEEE Electron Device Lett., vol. 36, no. 9, pp. 957–959, 2015.

[4] A. Guedes, S. Shelton, R. Przybyla, I. Izyumin, B. Boser, and D. A. Horsley, "Aluminum nitride pMUT based on a flexurally-suspended membrane," in 16th International Solid-State Sensors, Actuators and Microsystems Conference, 2011, pp. 2062–2065.

[5] E. Ledesma, I. Zamora, F. Torres, A. Uranga, V. Tzanov, and S. Bhd, "AlN piezoelectric micromachined ultrasonic transducer array monolithically fabricated on top of pre-processed CMOS substrates," in 2019 20th International Conference on Solid-State Sensors, Actuators and Microsystems & Eurosensors XXXIII (TRANSDUCERS & EUROSENSORS XXXIII), 2019, no. June, pp. 655–658.

[6] E. Ledesma et al., "AlN PMUT with crossed-cavity for better acoustic pressure outputs in liquid at high frequency," in 2019 20th International Conference on Solid-State Sensors, Actuators and Microsystems & Eurosensors XXXIII (TRANSDUCERS & EUROSENSORS XXXIII), 2019, no. June, pp. 825–828.

[7] E. Ledesma et al., "Squared PMUT with enhanced pressure sensitivities," in Eurosensors 2018, 2018, p. 925.

[8] M. Olfatnia, Z. Shen, J. M. Miao, L. S. Ong, T. Xu, and M. Ebrahimi, "Medium damping influences on the resonant frequency and quality factor of piezoelectric circular microdiaphragm sensors," J. Micromechanics Microengineering, vol. 21, no. 4, 2011.

[9] Q. Wang, G. L. Luo, Y. Kusano, and D. A. Horsley, "Low Thermal Budget Surface Micromachining Process for Piezoelectric Micromachined Ultrasonic Transducer Arrays With in-Situ Vacuum Sealed Cavities," in Hilton Head Workshop 2018: A Solid-State Sensors, Actuators and Microsystems, 2018, no. June, pp. 245–248.